

Supporting Information

Multi-functional Nanomodulators Regulate Multiple Pathways to Enhance Antitumor Immunity

*Yadan Zheng[†], Zhanzhan Zhang[†], Qi Liu[†], Yu Zhao[†], Chunxiong Zheng[†],
Jialei Hao[†], Kaikai Ye[§], Ying Wang[†], Chun Wang[†], Xinzhi Zhao[†], Linqi Shi^{*†},
Chunsheng Kang^{*§} and Yang Liu^{*†}*

[†] State Key Laboratory of Medicinal Chemical Biology, Key Laboratory of Functional Polymer Materials of Ministry of Education, College of Chemistry, Nankai University, National Demonstration Center for Experimental Chemistry Education, Nankai University, Tianjin, 300071, China. E-mail: shilinqi@nankai.edu.cn; yliu@nankai.edu.cn

[§] Tianjin Neurological Institute, Key Laboratory of Post-neurotrauma Neuro-repair and Regeneration in Central Nervous System, Ministry of Education and Tianjin City, Department of Neurosurgery, Tianjin Medical University General Hospital, Tianjin 300052, China, E-mail: kang97061@tmu.edu.cn

Table of Contents

<i>Materials</i>	S3
<i>Instruments</i>	S3
<i>Synthesis of 2-(Hexamethyleneimino)ethyl methacrylate monomers</i>	S4
<i>Synthesis of MSN</i>	S4
<i>Cell culture</i>	S5
<i>In vitro cytotoxicity analysis of MFNM</i>	S5
<i>Pharmacokinetic studies of MFNM</i>	S5
<i>In vivo biodistribution of MFNM</i>	S6
<i>In vivo toxicity of MFNM</i>	S6
<i>Immunofluorescence staining</i>	S6
<i>Cytokine detection</i>	S7
<i>Statistical Analysis</i>	S7
<i>References</i>	S18

Materials

2-(Hexamethyleneimino) ethanol (C7A), cetyltrimethylammonium chloride (CTAC), 1-ethyl-3-(3-dimethylaminopropyl)carbodiimide hydrochloride (EDC•HCl) *N*-hydroxysuccinimide (NHS) were purchased from Energy Chemical (Shanghai, China). Trimethylamine, tetraethoxysilane (TEOS, 98%), *N*-(3-Aminopropyl)-methacrylamine hydrochloride (Apm), *N*, *N*'-methylene bisacryamide (Bis), ammonium persulfate (APS), tetramethylethylenediamine (TEMED) and sodium acetate trihydrate (NaAc•3H₂O) were purchased from Aladdin (Tianjin, China). 3-methacryloxypropyltrimethoxysilane, methacryloyl chloride, and 2-methacryloyloxyethyl phosphorylcholine (MPC) were purchased from Heowns (Tianjin, China). phalloidin FITC, paraformaldehyde, and 4,6-diamidino-2-phenylindole dihydrochloride (DAPI) were purchased from Invitrogen (USA). Cy5-NHS and Cy3-NHS were obtained from Oukainasi Tech Inc. (Beijing, China). Antibody for flow cytometry and confocal laser scanning microscope observation (CLSM) were purchased from Invitrogen and Biolegend (USA). All ELISA kits were obtained from Elabscience (China). Mouse melanoma cells B16F10 was purchased from American Type Culture Collection (ATCC). Trypsin, fetal bovine serum (FBS) and RPMI 1640 culture medium were purchased from Sigma-Aldrich (Shanghai, China). THF, HCl, methanol and other chemical reagents were purchased from local chemical companies.

Instruments

Dynamic light scattering (DLS) and zeta potential measurements were performed on a Brookhaven ZETAPALS/BI-200SM (Brookhaven Instrument, USA). Transmission electron microscopy (TEM) observations were performed on a Talos F200C electron microscope at an acceleration voltage of 120 kV. ¹H nuclear magnetic resonance (¹H NMR) spectra were obtained on a Varian UNITY-plus 400 M NMR spectrometer. Fluorescence spectra were measured on Hitachi F4600. UV-Visible spectra were acquired with a NanoDrop One^c (Thermo Scientific, USA). Ultraviolet absorption was measured on a Tecan Spark plate reader. Flow cytometry analysis was performed on a

Guava easyCyte 8HT flow cytometry. Confocal laser scanning microscope (CLSM) images were captured on a FluoView Confocal Laser Scanning Microscopes-FV1000.

Synthesis of 2-(Hexamethyleneimino)ethyl methacrylate monomers

Synthesis of 2-(Hexamethyleneimino)ethyl methacrylate (C7A-MA) is described as a representative procedure.¹ First, 2-(pentamethyleneimino)ethanol (14.3 g, 0.1 mol), triethylamine (10.1 g, 0.1 mol), and hydroquinone (0.11 g, 0.001 mol) were dissolved in 100 mL THF. Methacryloyl chloride (10.4 g, 0.1 mol) was then added dropwise into a three-neck flask within 30 min at 0°C. The reaction mixture was stirred at room temperature overnight. After the reaction, the mixture was filtered to remove the precipitate. After the solvent was removed under reduced pressure, the residue was purified by silica gel chromatography (light petroleum/ethyl acetate= 5/1, v/v) to yield C7A-MA as a yellow liquid. Yield: 68%.

¹H NMR (400 MHz, CDCl₃, 25 °C, TMS, δ): 6.09 (br, 1H, CHH=C(CH₃)-), 5.55 (br, 1H, CHH=C(CH₃)-), 4.24 (t, *J* = 6.5 Hz, 2H, -OCH₂CH₂N-), 2.84 (t, *J* = 6.5 Hz, 2H, -OCH₂CH₂N-), 2.72 (m, 4H, -N(CH₂CH₂CH₂)₂), 1.94 (s, 3H, CH₂=C(CH₃)-), 1.63 (m, 4H, -N(CH₂CH₂CH₂)₂), 1.58 (m, 4H, -N(CH₂CH₂CH₂)₂) (Figure S2).

Synthesis of MSN

In a typical synthesis,² 53.4 g of DI-water, 6.24 g of CTAC, and 0.3 g of NaAc•3H₂O were mixed and stirred at temperature of 40°C for 2 h. Then 4.35 mL of TEOS was added into the mixture dropwise within 3 min under steadily stirring at 500 RPM. The solution was stirred for 24 h. After cooling to room temperature, the solution was centrifuged at 13,000 RPM for 25 min to isolate the products from the suspension. After washing with water for 3 times, the products were refluxed for 3 h with a 1 wt% solution of sodium chloride (NaCl) in methanol at room temperature to remove the CTAC. Then the obtained MSN (100 mg) suspended in ethanol was reacted with 3-methacryloxypropyltrimethoxysilane (0.5 mL) at room temperature in the dark overnight. The obtained nanoparticles were separated through centrifugation, washed several times with ethanol.

Cell culture

B16F10 cells and NIH 3T3 cells were obtained from American Type Culture Collection (ATCC) and cultured in RPMI 1640 with 10% (v/v) fetal bovine serum (FBS), 100 U mL⁻¹ penicillin and 100 mg mL⁻¹ streptomycin in an incubator (Thermo Scientific) at 37 °C under an atmosphere of 5% CO₂ and 90% relative humidity, respectively. The cells were sub-cultivated approximately every 2 days at 80% confluence using 0.25% (w/v) trypsin at a split ratio of 1:5.

In vitro cytotoxicity analysis of MFNM

The cytotoxicity of PM and MFNM were determined using CCK-8 viability assay. Briefly, cells (NIH 3T3 and B16F10) were seeded in 96-well plates at 5×10^3 cells per well and grown to 80% confluence, followed by replacing the culture medium with the fresh ones containing different nanoparticles at varied concentrations for further 24 h incubation. CCK-8 was mixed with RPMI 1640 at a volume ratio of 1/9 to achieve the CCK-8 working solution. After the incubation, the cells were rinsed with PBS, followed by the addition of 100 μ L CCK-8 working solution for additional 2 h incubation. Quantification of the cell viability was achieved by measuring the absorbance with Tecan's Infinite M200 microplate reader ($\lambda = 450$ nm). The cell viability was calculated by referring to the absorbance of the cells without any treatment.

Pharmacokinetic studies of MFNM

To investigate the pharmacokinetic of MFNM, female C57BL/6J (6~8 weeks of age) mice were purchased from SPF Experimental Animal Technology Co., Ltd. All experimental protocols were conducted within Nankai University guidelines for animal research and were approved by Institutional Animal Care and Use Committee. The mice were injected intravenously with Cy5 labeled nanoparticles, following by collecting the blood samples (40 μ L) at different times. The concentration of MFNM in blood was quantitatively examined by detecting the fluorescent intensity at 670 nm excited at 633 nm.

In vivo biodistribution of MFNM

The tumor-bearing mice were generated by subcutaneous injection of B16F10 cells (5×10^5 for each mouse) in the right leg of C57BL/6 mice at 6 weeks old. The mice were randomly divided into different groups. When the tumor volume was about 250 mm³, the mice were intravenously injected with 100 μ L of PBS, Cy5-nonPMPC-NP, Cy5-MFNM. At 24 h post-injection, the mice were sacrificed, and the major organs and the tumors were collected for *ex vivo* imaging. *Ex vivo* images were taken by IVIS Lumina imaged system (Caliper Life Sciences, USA). The fluorescence images were analyzed using Living Image 3.1 (Caliper Life Sciences, USA).

In vivo toxicity of MFNM

Female C57B6/L mice at 6-week old were administrated intravenously with PBS and MFNM for 7 days through tail vein. At the end of experiment, the mice from each group were sacrificed, and the blood were collected for blood chemistry analysis and blood routine analysis. The tests were performed using auto biochemistry analyzer and auto hematology analyzer, respectively. Major organs of the mice, including the hearts, the livers, the spleens, the lungs and the kidneys were collected, subsequently preserved in 4% buffered formaldehyde and embedded in paraffin. The paraffin sections were stained for examining the organ damage using H&E staining.

Immunofluorescence staining

For immunofluorescence studies, tumor tissues were immersed in 4% buffered formalin phosphate solution for 24 h, and then transferred to sucrose solution for dehydration. The tissues were then embedded in optimal cutting medium (O.C.T.), and frozen slices were made on a cryostat microtome. Immunofluorescence staining was performed by rinsing the slices with PBS, permeabilization, and blocking in 5% BSA solution at room temperature for 1 h. For the phenotype staining of T cells and Tregs, the fixed tumor sections were incubated with primary antibodies of CD4 (rat), CD8 (rabbit) and Foxp3 (rat), following by incubating with Alexa Fluor 488 conjugated second antibody and Alexa Fluor 594 conjugated second antibody. DAPI was used for nuclear

counterstaining. CLSM images were captured on an Olympus CLSM with a 20× emersion objective.

Cytokine detection

The intratumor levels of TGF- β , IFN- γ , TNF- α and IL-12 were measured with ELISA kits according to the manufacturer's instructions. All of these experiments were performed in triplicate.

Statistical Analysis

Statistical comparisons were achieved using one-way ANOVA with Dunnett post-test with GraphPad Prism 7.0. Data represent mean \pm standard error of the mean (s.d.) deviation from at least three independent experiments ($n \geq 3$) and the significance levels are * $p < 0.05$, ** $p < 0.01$, *** $p < 0.001$ and **** $p < 0.0001$

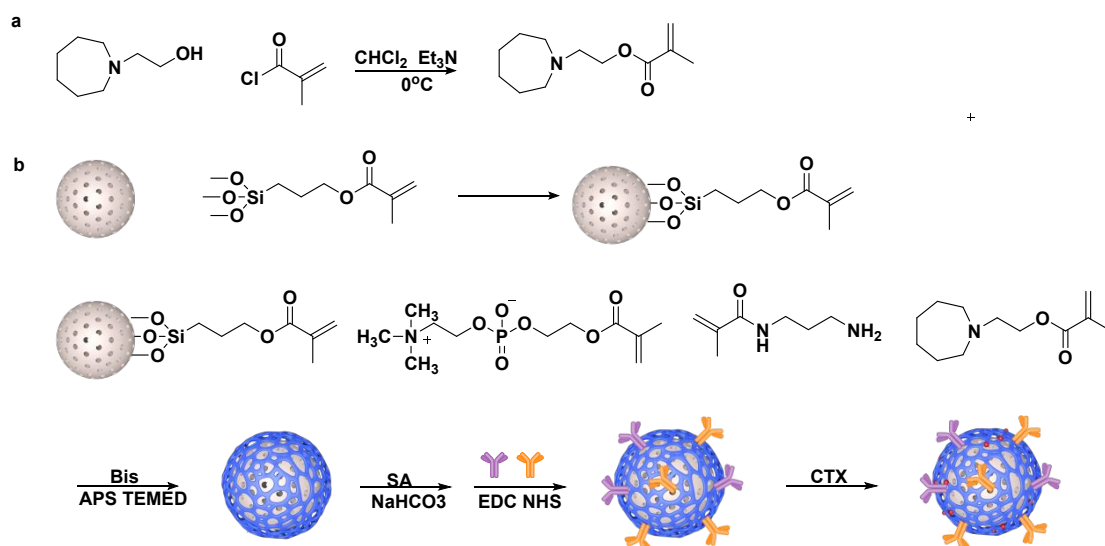


Figure S1. a) Synthesis routes of C7A-MA and b) schematic illustration of the MFNM synthesis.

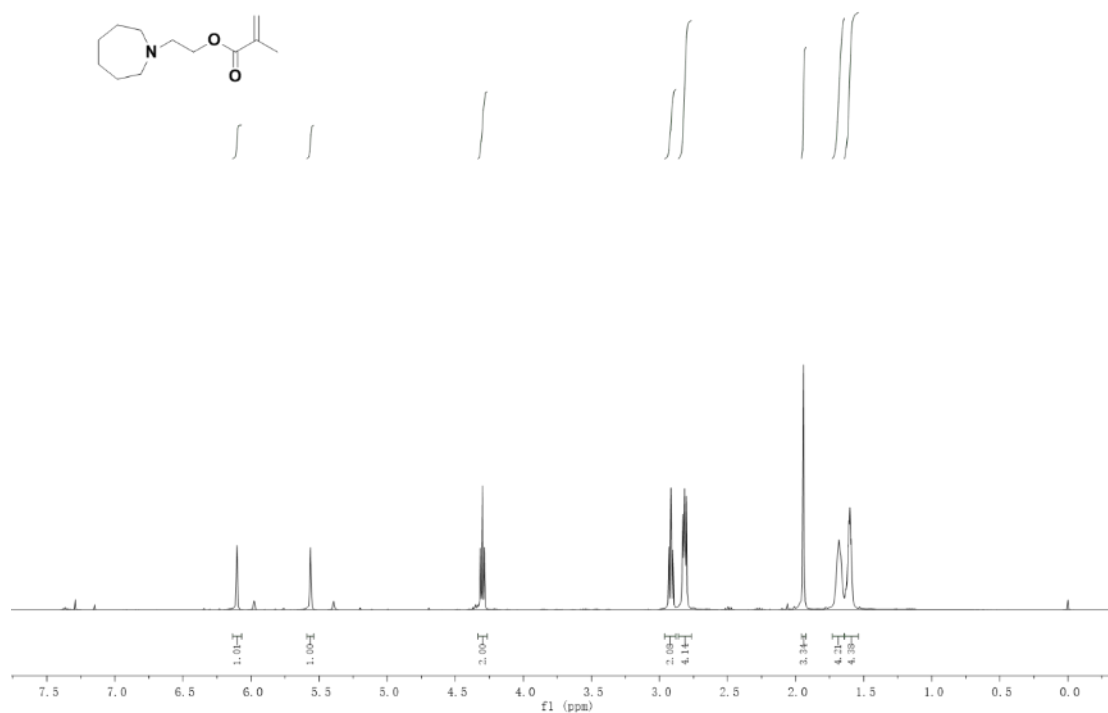


Figure S2. ^1H NMR spectra of 2-(Hexamethyleneimino) ethyl methacrylate (C7A-MA) in CDCl_3 .

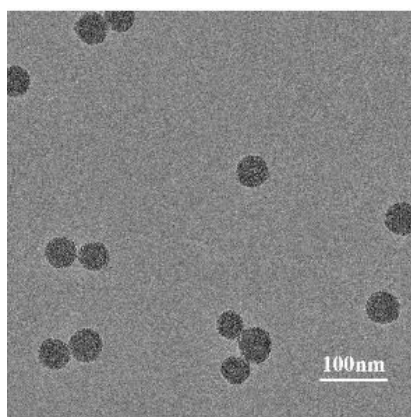


Figure S3. Morphology assessment of MSN using transmission electron microscopy (TEM) bright field. The scale bar represents 100 nm.

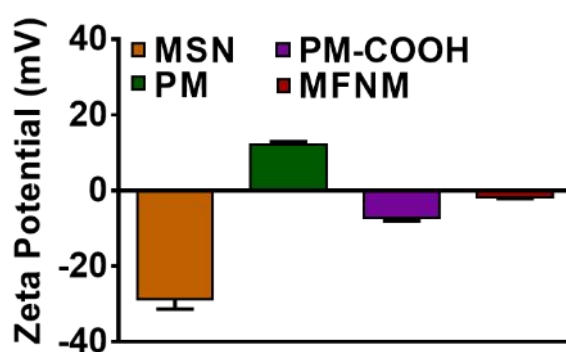


Figure S4. Zeta potential of MSN, PM, PM-COOH and MFNM. Data represent mean \pm standard derivations (s.d.) from three independent experiments ($n = 3$).

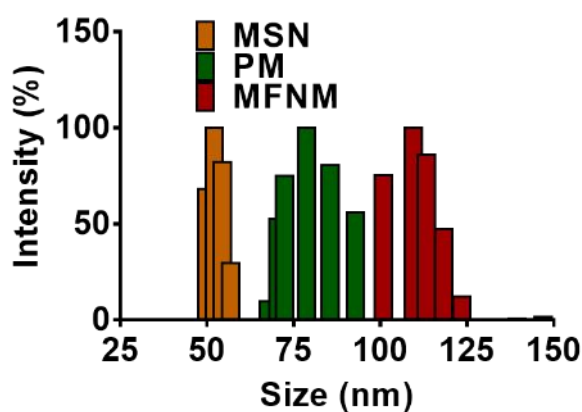


Figure S5. Hydrodynamic size distributions of MSN, PM, MFNM measured using dynamic light scattering (DLS).

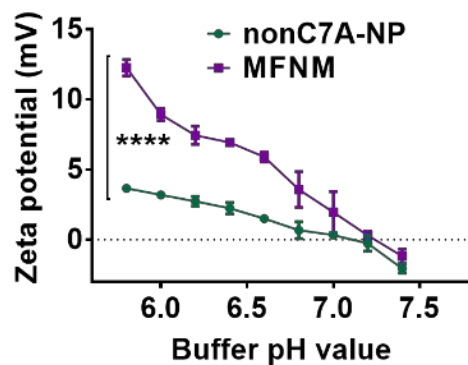


Figure S6. Zeta potential of nonC7A-NP and MFNM at different pH condition. Data represent mean \pm s. d. from three independent experiments ($n = 3$).

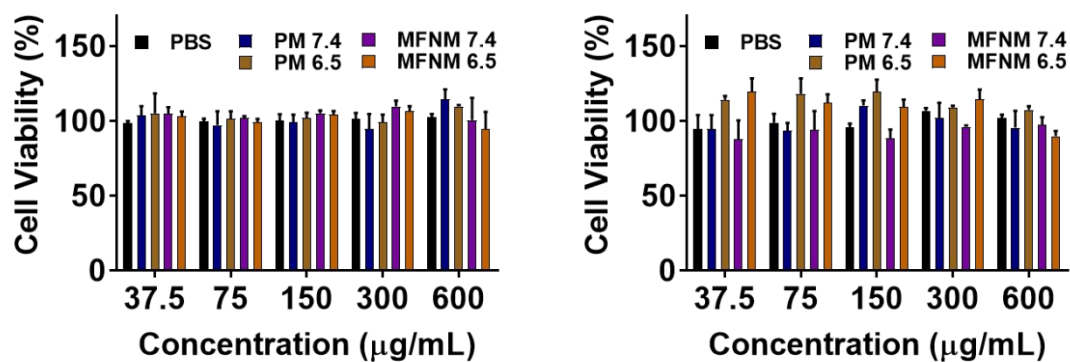


Figure S7. Cell viability of NIH 3T3 cells and B16F10 cells after treating with PM and MFNM at pH 7.4 and pH 6.5 for 24 h incubation. Cell viability was assessed using CCK-8 assay. All data are presented as mean \pm s.d. from three independent experiments ($n = 3$).

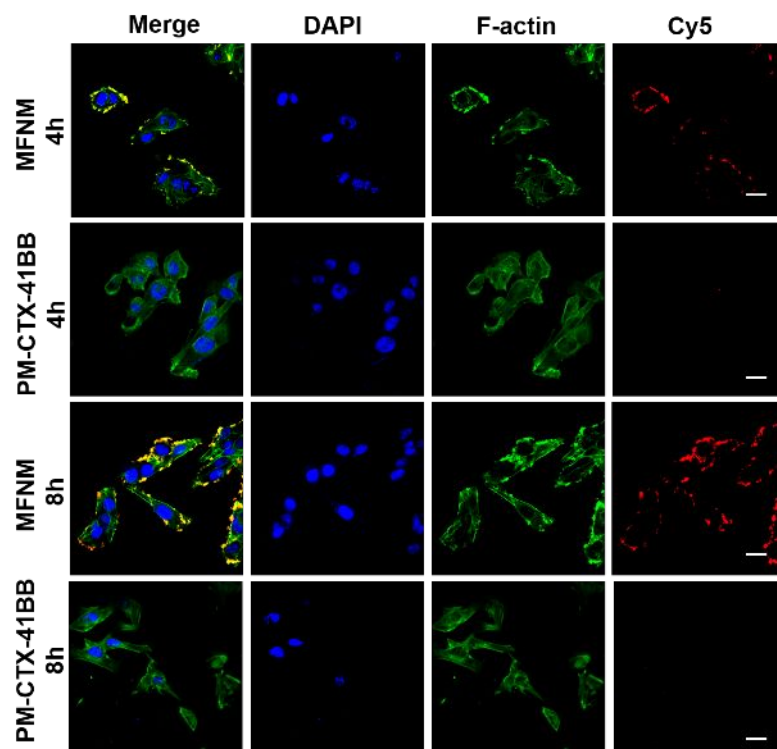


Figure S8. Confocal laser scanning microscope (CLSM) images of B16F10 cells after 4 h and 8h incubation with the Cy5-labeled MFNM and the Cy5(red)-labeled PM-CTX-41BB. Cellular nuclei and cytoskeleton F-actin were stained with DAPI (blue) and Phalloidin FITC (green), respectively. The scale bar represents 40 μm .

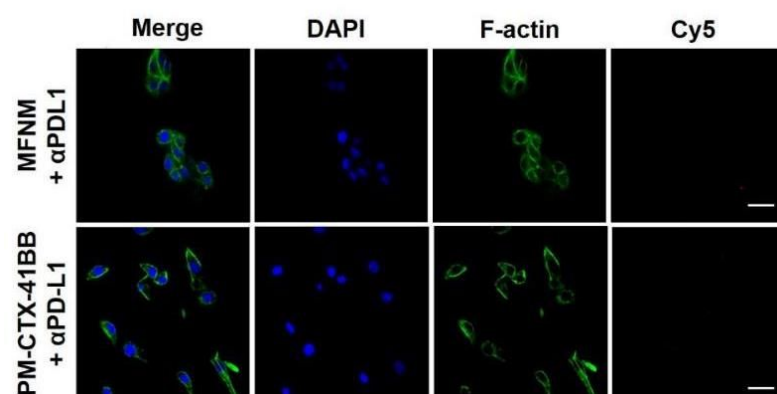


Figure S9. Confocal laser scanning microscope images (CLSM) of B16F10 cells treated with anti-PD-L1 mAbs prior to an incubation with the Cy5(red)-labeled PM-CTX-41BB and MFNM. Cells were stained with DAPI (blue) and Phalloidin FITC (green). The scale bar represents 20 μm .

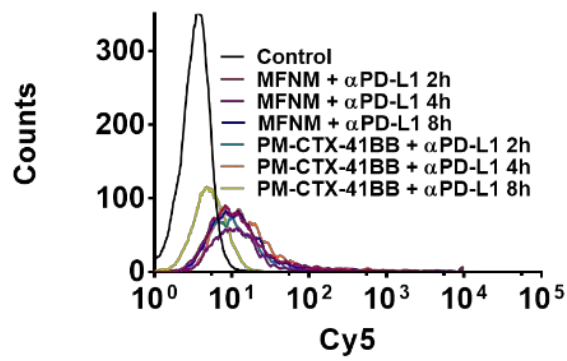


Figure S10. Flow cytometry profiles of B16F10 tumor cells pre-treated with anti-PD-L1 mAbs prior to an incubation with Cy5(red)-labeled PM-CTX-41BB, MFNM at 37 °C for 2h, 4h and 8h.

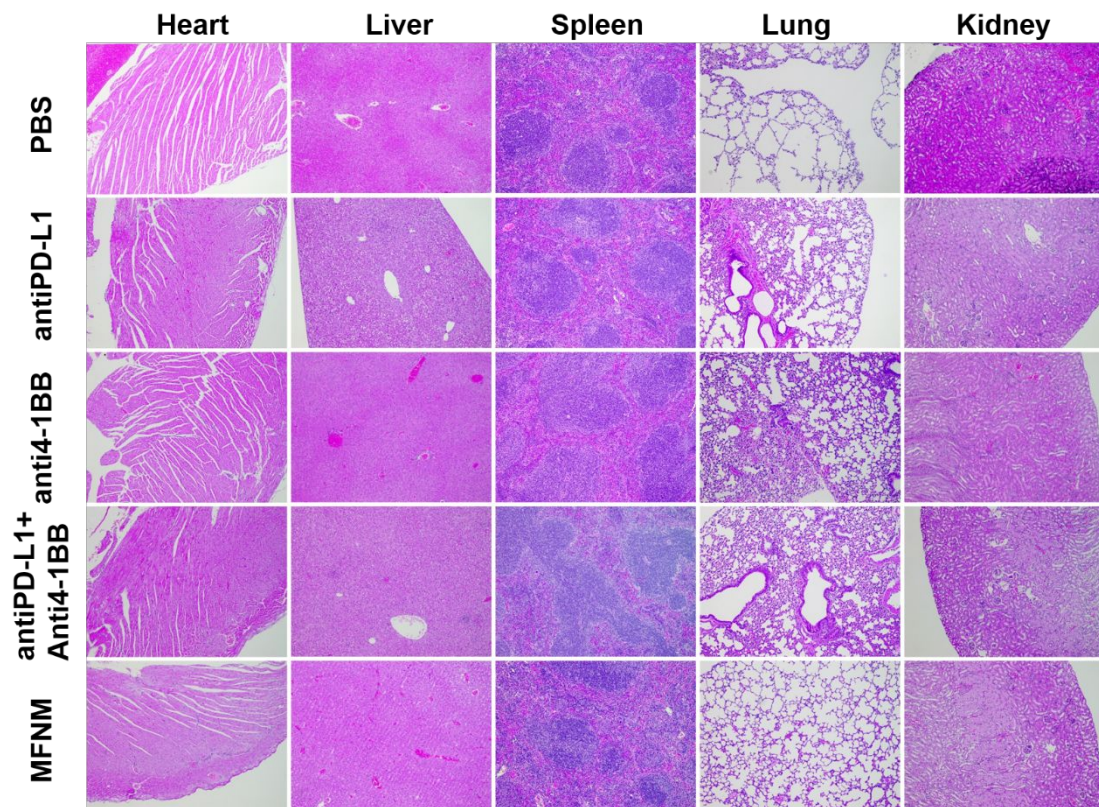


Figure S11. H&E staining tissue sections from the heart, the liver, the spleen, the lung and the kidney from the mice with PBS and MFNM.

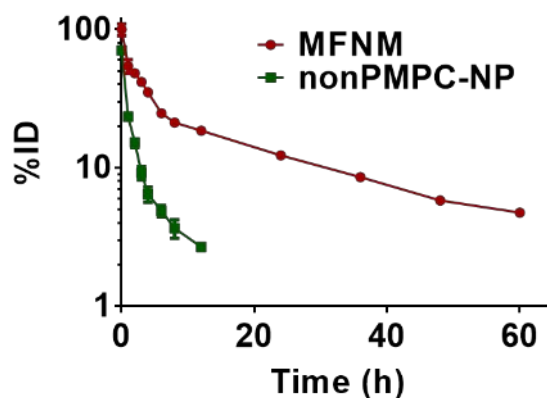


Figure S12. Pharmacokinetic curves of nanoparticles in mice after tail vein injection. Nanoparticles were pre-labelled with Cy5. Data represent mean \pm s.d. from three independent experiments ($n = 3$).

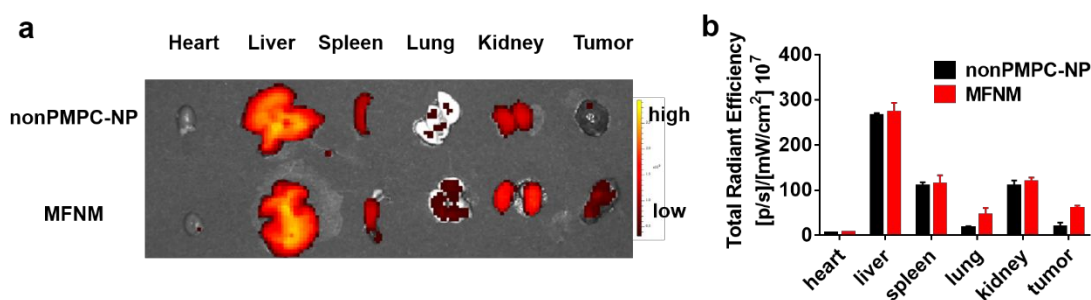


Figure S13. a) *Ex vivo* fluorescence imaging of the tumor and normal tissues harvested from the euthanized B16F10 tumor-bearing mice at 24 h post injection. **b)** Quantitative analysis of organ accumulation of nonPMPC-NP and MFNM based on the fluorescence intensity from the *ex vivo* images. Data represent mean \pm s.d. from three independent experiments ($n = 3$).

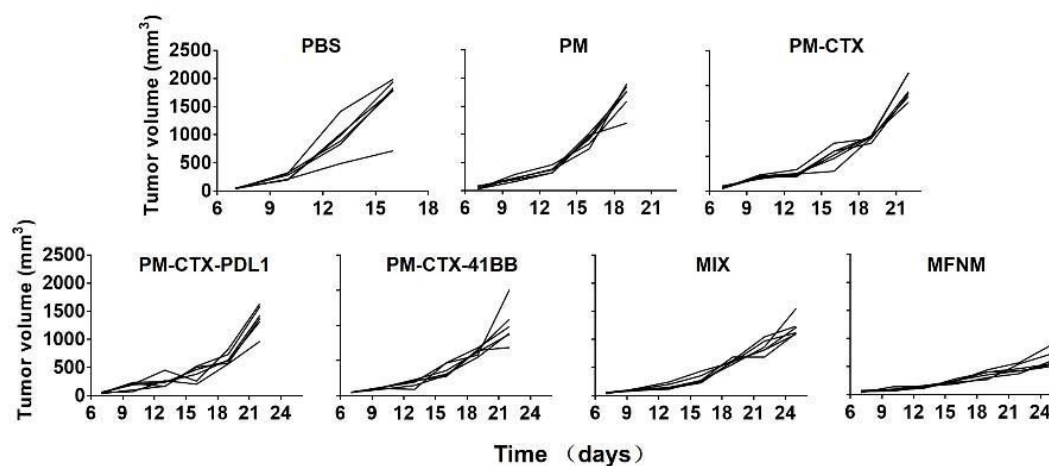


Figure S14. Individual tumor growth kinetics in different groups. Growth curves were stopped when the first mouse of the corresponding group died. Data represent mean \pm s.d. from six independent experiments ($n = 6$)

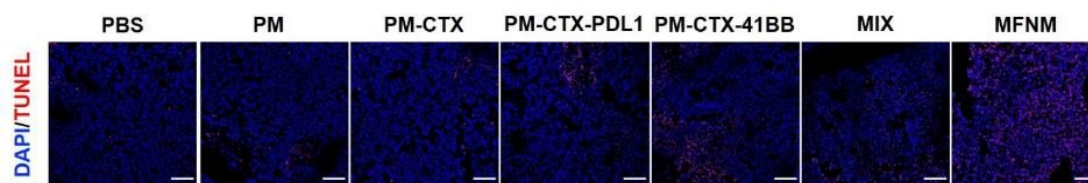


Figure S15. TUNEL analysis from the mice in tumor tissues treated with PBS, PM, PM-CTX, PM-CTX-41BB, PM-CTX-PDL1, MIX and MFNM. The scale bar represents 100 μ m.

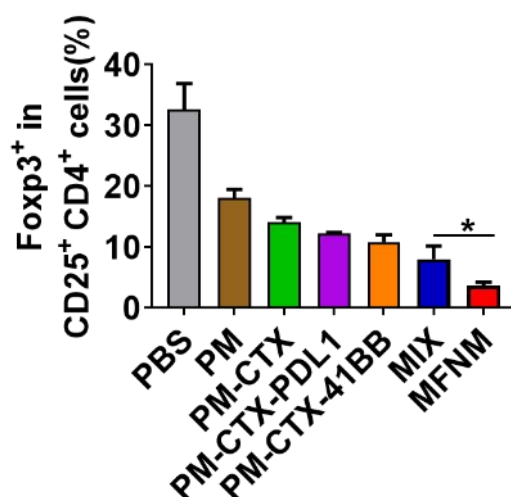


Figure S16. Flow cytometric analysis of the Tregs population within the tumor (gating on CD45⁺CD4⁺) at day 10 post-treatment. Data are presented as mean \pm s.d. from three independent experiments ($n = 3$).

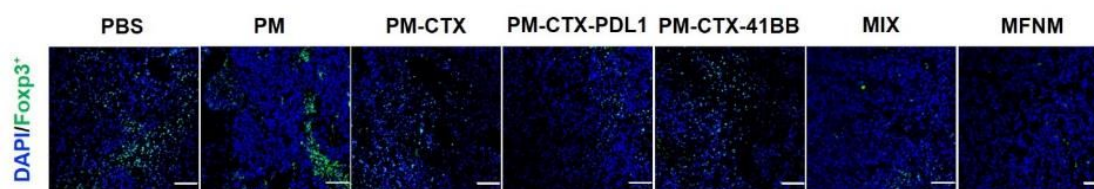


Figure S17. Representative immunofluorescence images of tumors showing Tregs infiltration in tumor tissues treated with PBS, PM, PM-CTX, PM-CTX-41BB, PM-CTX-PDL1, MIX and MFNM. The scale bar represents 100 μ m.

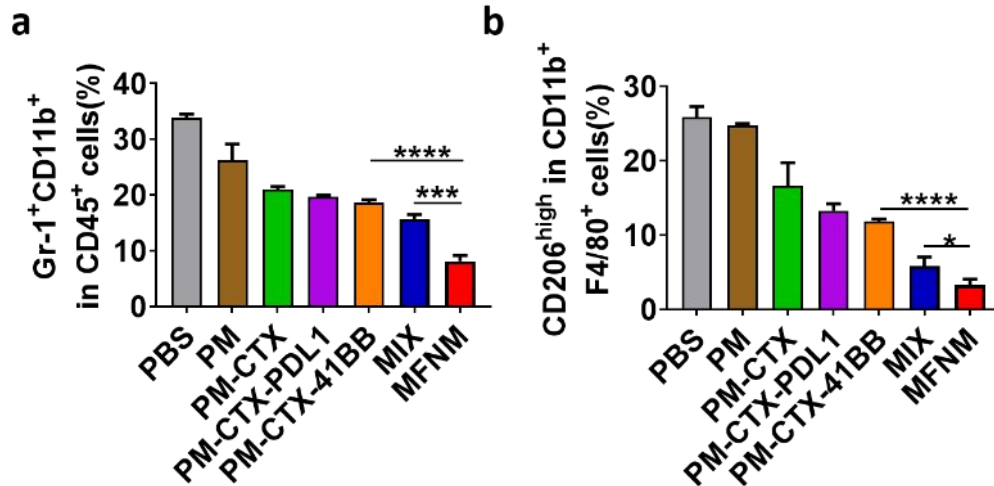


Figure S18. Flow cytometric analysis of MDSC **a**) infiltration within the tumor and the TAM **b**) infiltration within the tumor at day 10 post-treatment. Data are presented as mean \pm s.d. from three independent experiments ($n = 3$).

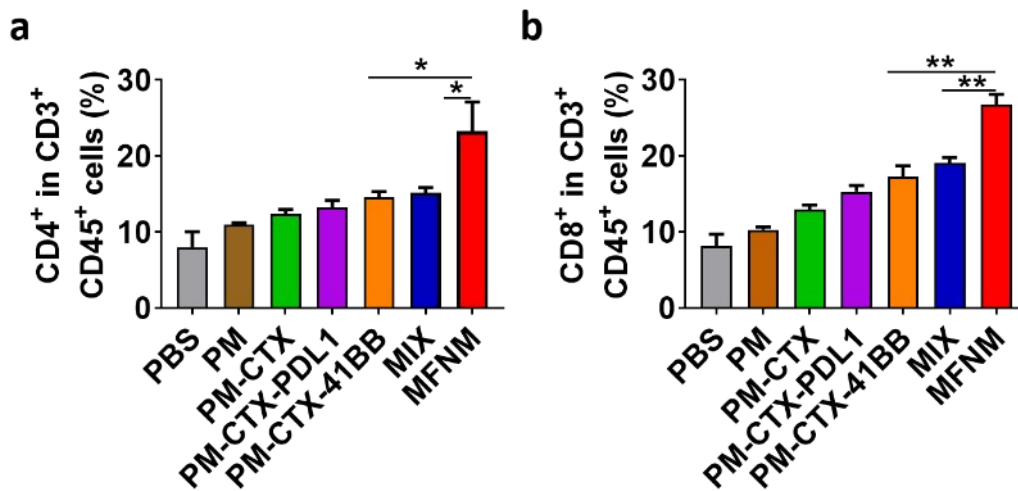


Figure S19. Flow cytometry analysis of the population of CD4⁺ T cells **a**) and CD8⁺ T cells **b**) within the tumor at day 10 post-treatment. Data are presented as mean \pm s.d. from three independent experiments ($n = 3$).

Table S1. Optimization of MFNM conjugation chemistry

Sample	Incubation($\mu\text{g}/\text{mg}$)	Feeding	[Conjugation]($\mu\text{g}/\text{mg}$)		Conjugation
	$[\alpha\text{PDL1}]:[\alpha\text{41BB}]$	Ratio	$[\alpha\text{PDL1}]$	$[\alpha\text{41BB}]$	Ratio
1	100:100	1:1	33.50	30.67	1.09
2	200:100	2:1	29.63	35.70	0.83
3	100:200	1:1	27.75	27.07	1.01
4	200:200	2:2	31.63	34.47	0.92

Table S2. Blood routine analysis in blood samples of C57BL/6 mice on 7 days after treatment

Group	WBC	RBC	PLT	HGB
	($10^9/\text{L}$)	($10^{12}/\text{L}$)	($10^9/\text{L}$)	(g/L)
PBS	4.6 \pm 0.14	8.2 \pm 0.33	1060 \pm 42.4	131.5 \pm 6.4
antiPD-L1	6.5 \pm 0.6	8.7 \pm 1.4	692 \pm 223.4	135.5 \pm 21.9
anti4-1BB	3.33 \pm 0.8	8.4 \pm 1.7	625.3 \pm 126.9	127.7 \pm 29.8
antiPD-L1 + anti4-1BB	1.9 \pm 0.55	6.5 \pm 0.5	398. 1 \pm 74.2	97.3 \pm 7.5
MFNM	6.9 \pm 3.5	7.3 \pm 1.9	810 \pm 135.1	114 \pm 21.7

Table S3. Values of serum enzymes in blood samples of C57BL/6 mice on 7 days after treatment

Group	AST (U/L)	ALP (U/L)	ALT (U/L)	BUN (mmol/L)
PBS	59.5±6.15	153.7±7.63	293.35±4.158	10.43±0.74
antiPD-L1	60.15±13.3	209.9±18.5	209.6±47.8	8.48±0.94
anti4-1BB	71.7±9.34	172.5±18.3	226.17±26.8	11.25±1.13
antiPD-L1 + anti4-1BB	71.7±6.8	282.47±13.9	168.08±5.54	8.17±1.35
MFNM	67.15±1.48	177.87±16.9	274.65±14.78	10.39±1.5

Table S4. Comparison of the Intravenous Pharmacokinetic Parameters for nonPMPC-NP and MFNM.

Parameters	nonPMPC-NP	MFNM
t_{1/2} (h)	2.897	0.7027
AUC (U/L)	857	135
AMUC (U/L h)	15355	5233
CL (mL/h)	1.078	35.74
V_d (mL)	0.003	6.24
MRT (h)	17.917	3.876

References

- (1) Zhou, K.; Wang, Y.; Huang, X.; Luby-Phelps, K.; Sumer, B. D.; Gao, J., Tunable, ultrasensitive pH-responsive nanoparticles targeting specific endocytic organelles in living cells. *Angew Chem. Int. Ed. Engl.* **2011**, *50* (27), 6109-6114.
- (2) Yu, M.; Zhou, L.; Zhang, J.; Yuan, P.; Thorn, P.; Gu, W.; Yu, C., A simple approach to prepare monodisperse mesoporous silica nanospheres with adjustable sizes. *J. Colloid Interface Sci.* **2012**, *376* (1), 67-75.